Swine manure treatment by anaerobic membrane bioreactor with carbon, nitrogen and phosphorus recovery

Fan Bu, Shiyun Du, Li Xie, Rong Cao and Qi Zhou

ABSTRACT

Swine manure wastewater was treated in an anaerobic membrane bioreactor (AnMBR) that combined a continuous stirred tank reactor (CSTR) and a hollow-fiber ultrafiltration membrane, and the feasibility of ammonia and phosphorus recovery in the permeate was investigated. The AnMBR system was operated steadily with a high mixed liquor suspended solids (MLSS) concentration of 32.32 ± 6.24 g/L for 120 days, achieving an average methane yield of 280 mL/gVS_{added} and total chemical oxygen demand removal efficiency of 96%. The methane yield of the AnMBR is 83% higher than that of the single CSTR. The membrane fouling mechanism was examined, and MLSS and the polysaccharide contents of the extracellular polymeric substances were found to be the direct causes of membrane fouling. The effects of the permeation/relaxation rate and physical, chemical cleaning on membrane fouling were assessed for membrane fouling control, and results showed that a decrease in the permeation/relaxation rate together with chemical cleaning effectively reduced membrane fouling. In addition, a crystallization process was used for ammonia and phosphorus recovery from the permeate, and pH 9 was the optimal condition for struvite formation. The study has an instructive significance to the industrial applications of AnMBRs in treating high strength wastewater with nutrient recovery.

Key words | anaerobic membrane bioreactor, fouling mechanism, struvite precipitation, swine manure wastewater, treatment efficiency

Fan Bu
Shiyun Du
Li Xie (corresponding author)
Rong Cao
Qi Zhou
Key Laboratory of Yangtze River Water Environment,
Tongji University,
1239 Siping Road,
Shanghai 200092,
China
E-mail: *sally.xieli@tongji.edu.cn*

INTRODUCTION

Anaerobic digestion is an effective bio-process in high-strength wastewater treatment, reducing environmental hazards while simultaneously producing biogas to meet local energy needs. It has been widely applied for years to the treatment of organic waste, including animal manure. However, anaerobic digestion of animal manure has several potential drawbacks that account for its frequently poor efficiency and unsteady operation. Firstly, biodegradability of animal manure is lower than other organic wastes or energy crops (Weiland 2006). Previous studies showed that the organic matter of animal manure is incompletely degraded, a relatively high concentration of suspended solids (SS) remains in the anaerobically treated effluent and the chemical oxygen demand (COD) removal efficiency is only up to 75–80% (Nasir *et al.* 2012). Secondly, the high nitrogen content in animal manure leads to a high concentration of ammonia in the reactor, which may in turn inhibit anaerobic digestion (Rajagopal *et al.* 2013).

Anaerobic membrane bioreactors (AnMBRs) are the combination of anaerobic digestion and microfiltration/ultrafiltration membranes, thereby achieving direct solid-liquid separation by the effective membrane interception of most microorganisms present in the system. Thus, the sludge retention time (SRT) is completely separated from hydrolytic retention time (HRT), and further degradation of organic matter with lower biodegradability can be enhanced. In recent years, the feasibility and process optimization of swine manure wastewater treatment with AnMBRs have been studied, mostly in systems incorporating tubular or flat membranes (Lee *et al.* 2001; Padmasiri *et al.* 2007). A stable performance, with 90% COD removal efficiency, was obtained using an external tubular

doi: 10.2166/wst.2017.278

ultrafiltration membrane with the flux in the range of 5–10 L/m^2/h and cross-flow velocities of up to 2 m/s. However, while the increase in cross-flow velocity benefited membrane performance, it resulted in poor anaerobic digestion (Padmasiri *et al.* 2007). Lee and co-workers investigated the performance of an anaerobic reactor with a submerged membrane module in the treatment of swine manure wastewater, reporting a COD removal efficiency of 80% and a methane yield of 0.32 m^3/$kgCOD_{removed}$ (Lee *et al.* 2001). In that study, membrane fouling was controlled using a stainless-steel pre-filter and aeration cleaning, both of which contributed to the reactor's long period of steady operation. Recently, an expanded granular sludge bed with a submerged hollow-fiber membrane enabled the effective treatment of swine wastewater was reported, with a COD removal efficiency of 90% (Lopez-Fernandez *et al.* 2011). Moreover, the feasibility of using the hollow-fiber membrane in an anaerobic reactor was demonstrated by the successful treatment of other wastewaters characterized by a high concentration of solids, e.g., excess sludge (Xu *et al.* 2011; Dagnew *et al.* 2013). However, the membrane fouling mechanism and long-term operation strategy of AnMBRs with hollow-fiber membrane for swine manure treatment were not fully investigated. Besides, although the AnMBR process could intercept solids and improve the organic loading, the permeate still contains a certain amount of ammonia and phosphorus, and needs further treatment.

Here, in this study, we investigated the feasibility of treating swine manure wastewater in an AnMBR, and recovery of ammonia, phosphorus in the permeate for carbon, nitrogen and phosphorus recycling. The treatment efficiency, methane yield and optimal pH for struvite formation were determined. Our discussion includes an analysis of the strategies to control membrane fouling, a comparison of the performance and bacterial community structures between the AnMBR and continuous stirred tank reactor (CSTR) systems, and an evaluation of the role of the membrane in the anaerobic digestion process.

MATERIALS AND METHODS

Substrate

The swine manure used in this experiment was collected from a pig farm on Chongming Island, Shanghai, and stored at 0–4 °C before use. The raw swine manure was diluted ten-fold with tap water to simulate the typical wastewater washing procedure on the pig farm. Table 1 shows the characteristics of the swine manure wastewater, which is a typical high strength wastewater contained high concentrations of COD, SS and nitrogen. The seed sludge used in this study was mesophilic anaerobic granular sludge taken from an internal circulation reactor of a paper mill plant in Jiangsu, China. The concentration of the total suspended solids (TSS) and volatile suspended solids (VSS) in the seed sludge were 56.2 g/L and 45.7 g/L, respectively. The sludge was inoculated without pre-treatment.

Table 1 | Characteristics of the inflow

Parameter[a]	Value	Parameter[a]	Value
pH	7.6 ± 0.1	SCOD	3,705 ± 240
Total solids	10,850 ± 2,640	TN	743 ± 15
VS	7,945 ± 2,156	NH_4^+-N	250 ± 57
SS	10,206 ± 2,902	TP	–
VSS	7,521 ± 2,313	SOP	98 ± 13
TCOD	13,476 ± 2,238	VFA	1,722 ± 415

VS, volatile solids; SS, suspended solids; VSS, volatile suspended solids, TCOD, total chemical oxygen demand; SCOD, soluble chemical oxygen demand, TN, total nitrogen; TP, total phosphorus, SOP, soluble orthophosphate; VFA, volatile fatty acids.
[a]Except for pH, the units of all the other parameters are mg/L.

Experimental setup

Figure 1 shows a bench-scale AnMBR system combining an external submerged hollow-fiber ultrafiltration membrane with an anaerobic CSTR. The working volume/total volume of the CSTR and membrane module was 11 L/13 L and 3 L/3.5 L, respectively (as shown in Figure 1). The anaerobic reactor was operated at 35 °C. The contents were stirred using a mixer with a rotating speed of 100 rpm, controlled by the online PC control cabinet. The membrane module consisted of a polyvinylidene fluoride membrane and an external pressure type hollow-fiber membrane with a length of 175 mm, a diameter of 56 mm, a total surface area of 0.047 m^2, and a pore size of 0.04 μm. The upper limits of its operational transmembrane pressure (TMP), temperature, and aeration flow were 62 kPa, 40 °C, and 30 L/min, respectively; proper functioning is at a TMP between 10 and 50 kPa. An air pump was used to ensure continuous biogas blowing at 5.5 L/min to prevent membrane fouling. Biogas aeration was stopped after the daily discharge of the anaerobic digestate, and then the methane was collected for volume and composition analysis. Another CSTR system with the same volume was operated under the same conditions in order to compare the treatment efficiency of the two systems.

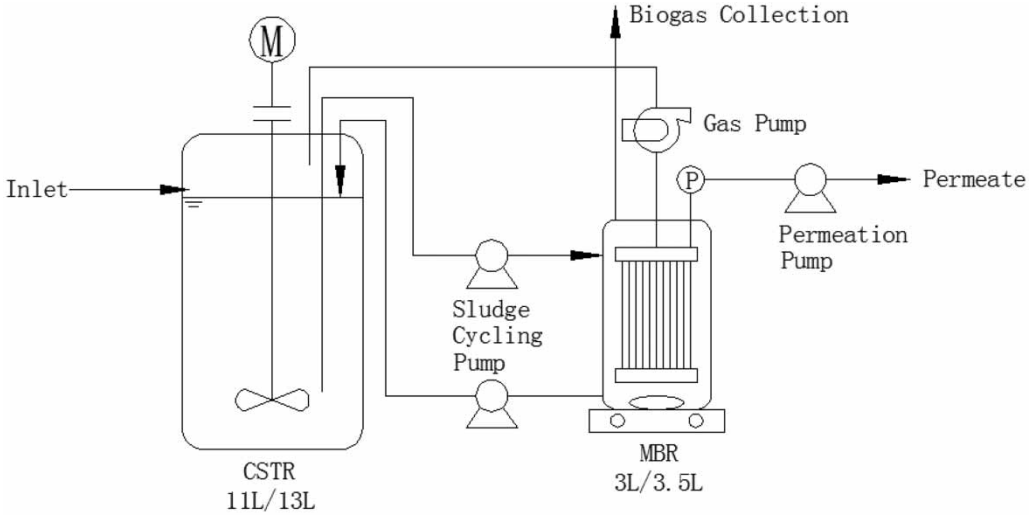

Figure 1 | Flow diagram of the AnMBR system.

Initially, the performance of the anaerobic CSTR without the membrane module in the treatment of swine manure was investigated with respect to biogas production and ammonia nitrogen accumulation. Table 2 lists the operational parameters for the AnMBR. Since the swine manure had a high SS concentration, it was difficult to pump it into the reactor continuously in our study. The AnMBR was operated under semi-continuous condition without pH control. The permeate/effluent was discharged once a day, and then fresh swine manure was added into the reactor. A recycling sludge pump was used for continuous sludge recycling between the CSTR and the AnMBR to ensure that a stable mixed liquor suspended solids (MLSS) concentration of 32.3 ± 6.2 g/L was reached. One hundred mL of sludge sample was removed daily, and 1–2 L of sludge was discharged after each physical cleaning of the system.

Ammonia and phosphorus in the permeate of the AnMBR was recovered as struvite by crystallization, and jar test was conducted for optimal conditions. The crystallization of the permeate was evaluated in the 1,000 mL beakers with 800 mL permeate at three pH (8, 9 and 10). The permeate was magnetically stirred with a rotating speed of 400 r/min for 30 min right after adjusting pH with 2 mM NaOH. The precipitate was filtered out and dried for 48 hours at 40 °C and then analysed for its weight and components. The ion concentrations (soluble orthophosphate (SOP), NH_4^+-N, Mg^{2+}, Ca^{2+}) of the filtrate was also analyzed for the calculation of recovery efficiency.

Table 2 | Operating parameters of the AnMBR

Parameter	Value	Parameter	Value
Feeding pattern	Semi-continuous inflow	Temperature	35 ± 0.5 °C
Membrane flux	3–5 L/(m^2·h)	pH	7.5 ± 0.4
OLR	1.17 ± 0.19 gCOD/(L·d)	HRT	13 d
MLSS	32.32 ± 6.24 g/L	SRT	45 d

OLR, organic loading rate; MLSS, mixed liquor suspended solids; HRT, hydraulic retention time; SRT, solids residence time.

Analytical methods and data processing

Chemical and microbial community analysis

The liquid samples were centrifuged at 10,000 rpm for 10 min and filtered immediately through 0.45-μm filters. TSS, VSS and SOP were analyzed in accordance with APHA *Standard Methods* (APHA 1998). Total and soluble chemical oxygen demand (TCOD and SCOD), total phosphorus (TP), total nitrogen (TN) and ammonia nitrogen (NH_4^+-N) were determined using a DRB200 and a DR2800 digital reactor block and the method described by the manufacturer (Hach Co., Colorado, USA). The pH value was detected using a EUTECH-510 gas electrode (California, USA).

Extracellular polymeric substances (EPS) were extracted from the sludge by thermal treatment (Wang *et al.* 2006) and soluble microbial products (SMP) were extracted from the liquid sample after filtration through 0.22-μm filters. The polysaccharide and protein contents of the EPS and SMP were analyzed using the phenol-sulfuric

acid method (calibrated against glucose) and Folin-Ciocalteu method (calibrated against bovine serum albumin), respectively. Volatile fatty acids (VFAs, C2–C5), biogas production, and biogas composition were determined as described in our previous publication (Wang *et al.* 2011). Metal ions were determined using Ion Chromatography (Dionex ICS-3000, Sunnyvale, CA, USA) as described in (Xie *et al.* 2012). The precipitate was analysed by X-ray diffraction scanning (XRD, RigakuD/max), scanning electron microscope (SEM) and energy dispersive spectrometer (EDS, Philips XL30 D6716).

High performance size exclusion chromatography (HPSEC) was employed to determine the apparent molecular weight distribution of the inflow, fermentation liquor and permeate. A gel filtration chromatography analyzer was used, which consisted of a TSK gel 4000SW column (TOSOH Corporation, Japan) and a liquid chromatography spectrometer (LC-10AD, Shimadzu, Japan). Polyethylene glycol (Merck Corporation, Germany) standards with different molecular weight were used for calibration. The elution at different time intervals was collected by an automatic fraction collector, and then analyzed automatically via a differential detector to obtain the molecular weight distribution.

The microbial community was collected from the sludge by centrifugation, and the analytical method was described in our previous publication (Wang *et al.* 2011). The primers used in this study were F340-GC (5′-CGC CCG CCG CGC GCG GCG GGC GGG GCG GGG GCA CGG GGG G CCC TAC GGG GYG CAS CAG-3′) and R519 (5′-TTACCG CGG CKG CTG-3′). The ~250-bp fragment of the V3 region of 16S rDNA was amplified in a polymerase chain reaction (PCR) using the primers. Sequence similarity searches were performed using the Basic Local Alignment Search Tool (BLAST). The results were used to search the National Center for Biotechnology Information sequence database (http://www.ncbi.nlm.nih.gov/BLAST/).

Data analysis

To characterize membrane fouling, with the goal of optimizing the operational parameters, the fouling rate of the membrane module was first calculated. The theoretical and experimental formulas of membrane fouling resistance (R_t) were summarized in a previous study (Meng *et al.* 2009). Rosenberger and co-workers corrected the formula for R_t described in Equation (1) by adding a temperature component. The resulting Equation (2) is appropriate for the analysis of a submerged membrane module (Rosenberger *et al.* 2006) and was used in the present work to calculate the apparent membrane fouling resistance:

$$R_t = \frac{TMP}{\eta J} \tag{1}$$

where η (Pa s) is the viscosity of the permeate, assumed to be the viscosity of pure water at a given temperature; TMP (Pa) is the trans-membrane pressure measured using a mercury manometer and J ($m^3 \cdot m^{-2} \cdot s^{-1}$) is the permeation flux through the membrane.

$$R_t = \frac{1}{\eta}\frac{TMP}{Jf_T} \tag{2}$$

$$f_T = e^{-0.0239(T-20)} \tag{3}$$

where f_T is the temperature correction parameter (Equation (3)); T (°C) is the temperature of the fermentation liquor and the remaining terms are as above. R_t was related to time (t) by linear fitting, with the slope of that line being the apparent membrane fouling resistance.

RESULTS AND DISCUSSION

Performance of the AnMBR system for swine manure treatment and carbon recovery by methane production

Figure 2 shows the performance of the AnMBR system in the treatment of swine manure wastewater, and carbon recovery was achieved by methane production. Biogas production, methane yield, and COD removal were measured during 120 days of operation. Under semi-continuous operation of the AnMBR system, the volume of biogas ranged from 3 to 5.3 L, with a production rate of about 5 L/d and a methane content of 60% (Figure 2(a)). As shown in Figure 2(c), the average COD removal efficiency was 96%, with the COD content of the permeate as low as 480 mg/L. In a previous study, in which swine manure wastewater was treated with a system comprising an anaerobic CSTR combined with a tubular membrane, similar results were reported; the average TCOD removal efficiency was >96% at an organic loading rate (OLR) of 1 g VS/(L·d) (Padmasiri *et al.* 2007). The pH of the AnMBR system in this study was maintained at about 7.8, and the alkalinity was maintained above 2,000 mg $CaCO_3$/L during 120 days of operation,

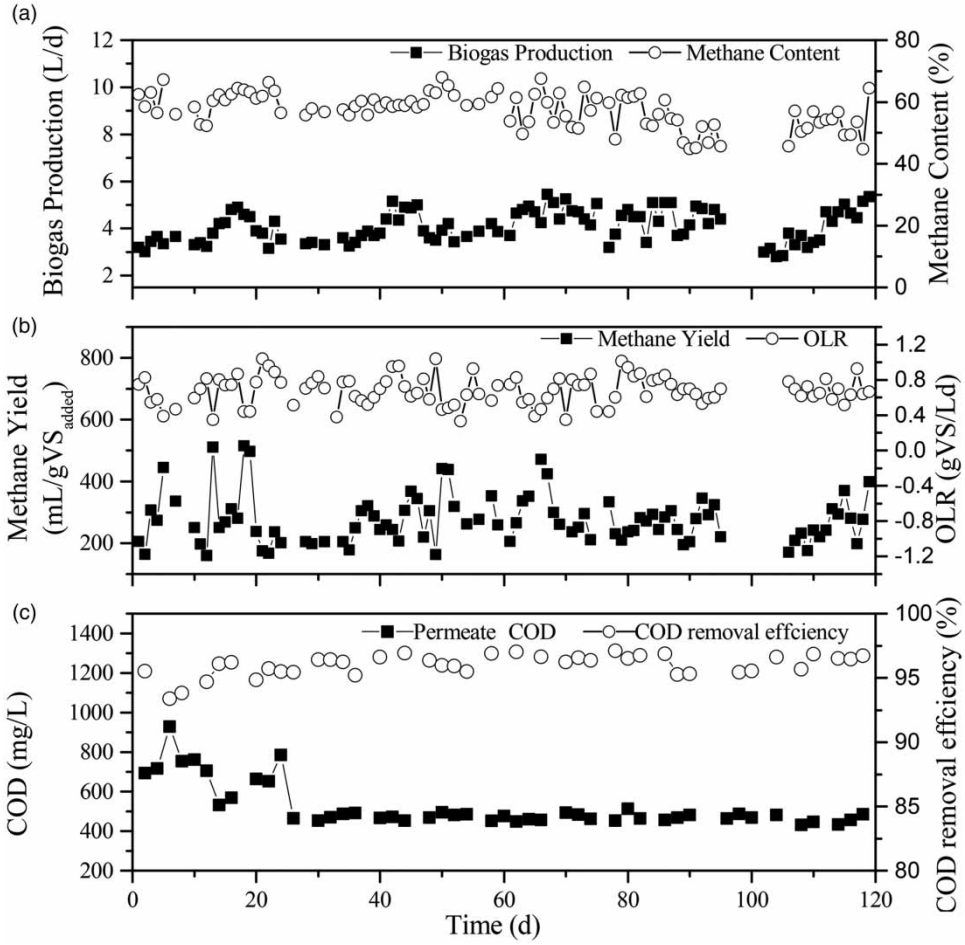

Figure 2 | Methane yield and COD removal: (a) biogas production and methane content; (b) methane yields according to the OLR; (c) COD concentration of the influent and permeate.

indicating the steady operation and strong buffering capacity of the anaerobic system.

The effluent quality and treatment efficiency of the CSTR were also compared to that of the AnMBR (Table 3). As shown, the COD concentration of the AnMBR effluent was much lower than that of the CSTR effluent. The permeate contained negligible amounts of TSS and VFAs, whereas the effluent from the CSTR (fermentation liquor) still contained 10.1 ± 0.7 g TSS /L and 30 mg VFAs /L. The above results indicated that the membrane module achieved effective interception and enhanced further degradation of organic matter, and the latter led to a methane yield of the AnMBR 83% higher than that of the CSTR. In addition, the ammonia nitrogen content of the permeate was similar to that of the fermentation liquor (495 and 485 mg/L, respectively); while the average SOP concentration was much lower (27.4 ± 9.0 and 51.8 ± 9.0 mg/L, respectively). These results further confirmed that interception by the membrane module played an important role in the AnMBR system.

Table 3 | Comparison of effluent quality and treatment efficiency between the CSTR and AnMBR system

	Parameter	CSTR	AnMBR
Effluent quality	COD (mg/L)	8,643 ± 841	491 ± 112
	SS (g/L)	10.1 ± 0.7	0
	VFA (mg/L)	30.4 ± 3.5	0
	NH_4^+-N (mg/L)	485 ± 43	495 ± 32
	SOP (mg/L)	51.8 ± 9.3	27.4 ± 9.0
Treatment efficiency	COD removal (%)	38 ± 6.9	96 ± 1.1
	Methane yield (mL/gVS_{added})	153 ± 64	280 ± 93

The molecular weight distribution of the influent, fermentation liquor and permeate of the AnMBR were compared to further understand the role of the membrane module. As seen in Figure 3, the molecular weights of the influent components were distributed in peaks 1, 2, 3, 5,

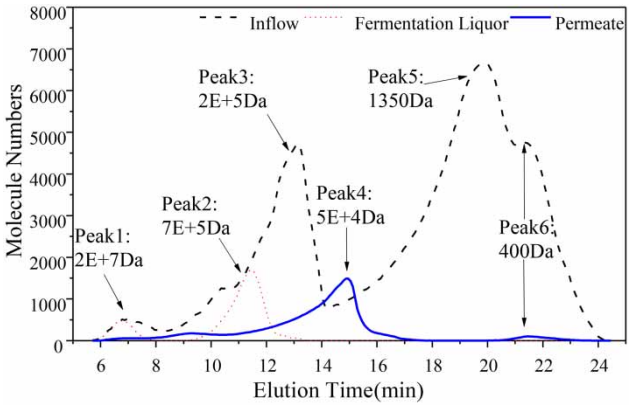

Figure 3 | Molecular weight distributions of the inflow, fermentation liquor and permeate.

and 6; those of the fermentation liquor in peaks 1 and 2; and those of the permeate in peaks 4 and 6. In a previous study, the macromolecular fraction corresponded to compounds with a molecular weight >4,000 Da and consisted of carbohydrates and proteins; the mid molecular weight fraction covered the range of 1,000–4,000 Da and included humic substances; and the low molecular weight fraction, <1,000 Da, mainly comprised cellular building blocks and organic acids (Lyko *et al.* 2008). Based on the differences in the molecular weight distribution between the fermentation liquor and the permeate, macromolecules with a molecular weight $>7\times10^5$ Da were intercepted by the membrane module. Compounds with a molecular weight of 5×10^4 Da appeared in the permeate but were absent in the fermentation liquor, perhaps because interception by the membrane module increased the contact time of the macromolecules and the microorganisms attached to the membrane, enabling the digestion of the former macromolecules into smaller compounds. The results thus indicated that most of the polysaccharides and proteins were biodegraded in the AnMBR, and that the reduced concentration of macromolecules in the permeate reflected their effective interception by the membrane module.

Microbial community analysis

To investigate how the addition of the membrane module affected the microorganisms within the reactor, the structures of the bacterial communities in the AnMBR system and CSTR system were analyzed. When the operational conditions in the two reactor systems had reached steady-state, the bacterial community was sampled and its structure subsequently analyzed by PCR-denaturing gradient gel electrophoresis (DGGE).

The results (Figure 4 and Table 4) showed that the bacteria in this study were mainly Firmicutes (bands 1, 7, 12, and 13), Bacteroidetes (bands 3 and 4), and Proteobacteria (bands 5, 6, 8 and 11), which is consistent with a full-scale anaerobic digester feeding with swine manure in Japan (Niu *et al.* 2015). The bacterial community structure in the AnMBR differed from the CSTR, and two members belonging to Bacteroidetes (band 3 and 4) that existed in the AnMBR were absent in the CSTR. Considering the short generation time of these two bacteria, the difference was not caused by longer SRT in the AnMBR than the CSTR. Sequencing results (Table 4) showed that bands 3 and 4 were closely related (99% similarity) to *Bacteroides propionicifaciens* and *Bacteroides graminisolvens* respectively. The former species produces propionic acids by decomposing saccharides (Ueki *et al.* 2008), while the latter mainly decomposes macromolecular polysaccharides such as xylan and starch (Nishiyama *et al.* 2009). A likely explanation for the presence of the additional Bacteroides species in the AnMBR is that interception of the microorganisms by the membrane module increased their contact time with the similar intercepted macromolecules and thereby supported macromolecular digestion by *Bacteroides propionicifaciens* and *Bacteroides graminisolvens* and thus their growth and enrichment. In a laboratory-scale continuously running fermentative hydrogen-producing membrane bioreactor, *Bacteroides* and *Clostridium* were the dominant genera, with the former predominant genera in the hydrolysis of organics (Shen *et al.* 2010).

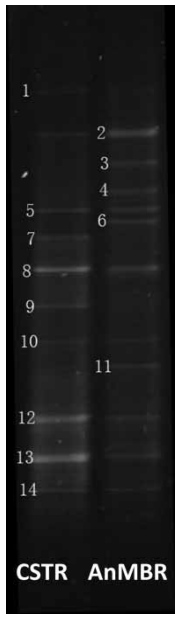

Figure 4 | Comparison of the bacterial community structure in the CSTR and AnMBR.

Table 4 | Sequences of the of 16S rDNA fragments obtained from DGGE

Microorganism	Band	Organism affiliation	Identify (%)	Phylum	Accession no.
Bacteria	1	*Syntrophomonas palmitatica*	99	Firmicutes	NR_041528.1
	3	*Bacteroides propionicifaciens*	99	Bacteroidetes	NR_041485.1
	4	*Bacteroides graminisolvens*	99	Bacteroidetes	NR_041642.1
	5	*Acinetobacter gyllenbergii*	97	Proteobacteria	NR_042026.1
	6	*Acidovorax delafieldii*	97	Proteobacteria	NR_028714.1
	7	*Carnobacterium divergens*	96	Firmicutes	NR_044706.1
	8	*Psychrobacter frigidicola*	99	Proteobacteria	NR_042222.1
	11	*Pseudomonas kilonensis*	99	Proteobacteria	NR_028929.1
	12	*Syntrophomonas curvata*	99	Firmicutes	NR_025752.1
	13	*Clostridium populeti*	98	Firmicutes	NR_026103.1
Archaebacteria	2	*Methanobacterium palustre*	100	Euryarchaeota	NR_041713.1
	9	*Methanosaeta thermophila*	100	Euryarchaeota	NR_028157.1
	10	*Methanoculleus marisnigri*	99	Euryarchaeota	NR_044723.1
	14	*Methanosaeta concilii*	99	Euryarchaeota	NR_028242.1

By contrast, according to the DGGE sequencing results, there was little different in the archaebacteria (methanogens) present in the two systems. As listed in Table 4, three bands (2, 10, and 14) corresponding to methanogens were obtained in the AnMBR. These were subsequently identified as *Methanobacterium palustre*, *Methanoculleus marisnigri* and *Methanosaeta concilii*. Those species together with *Methanosaeta thermophile* (band 9) were also detected in the CSTR. The slightly lower microbial diversity in the AnMBR suggests that *M. thermophile* was unable to adapt to the operational conditions of the system such that it gradually died out (Chen *et al.* 2009).

Membrane fouling and mechanism

The control of membrane fouling is essential for the successful long-term operation of the membrane module. The AnMBR was operated for 120 days under different flux conditions and permeation/relaxation rates. For the purpose of this study, the 120 day operation period was divided into seven stages according to the physical cleaning times. Physical cleaning was carried out by washing the membrane with water. As shown in Table 5, the fluxes of the hollow-fibre membrane ranged roughly between 3.0 and 5.1 L/(m^2·h) during stage 1–4, depending on the permeation/relaxation ratio of 10/1, in agreement with previous investigations of AnMBR system equipped with hollow-fiber membrane (Kim *et al.* 2011; Xu *et al.* 2011). And a similar flux of 3 L/(m^2·h) in the treatment of swine manure wastewater with an AnMBR fitted with a tubular membrane (Padmasiri *et al.* 2007). Figure 5 shows TMP and membrane flux variation under different operation conditions. Under the permeation/relaxation rate of 10/1 (stage 1–4), physical cleaning was carried out every 15 days, and the TMP of the membrane was returned to the initial value after physical cleaning. However, the TMP and membrane fouling

Table 5 | Operation parameters of the membrane module during seven stages of operation[a]

Stage	Flux (L/(m^2·h))	Intermittent ratio (min/min)	Operation time (d)	Membrane cleaning	Viscosity (Pa·s)	Fouling rate [×10^8 1/(m·day)]	$R_t \sim t$ (R^2)[b]
1	3.0	10/1	15	Physical	2.80	1.93	0.942
2	3.6	10/1	15	Physical	3.10	2.26	0.909
3	3.5	10/1	15	Physical	3.30	3.38	0.955
4	5.1	10/1	15	Physical	3.45	3.66	0.984
5[c]	5.8	10/1	15	Physical	3.44	1.29	0.964
6	5.6	5/1	20	Physical	4.12	0.85	0.946
7	3.9	10/1	20	Chemical	4.45	0.75	0.831

[a]According to the physical cleaning time.
[b]R^2 represents for the determination coefficient of the linear regression equation between membrane fouling resistance (Rt) and time (t).
[c]The AnMBR system was started rapidly again after a 40 day pause.

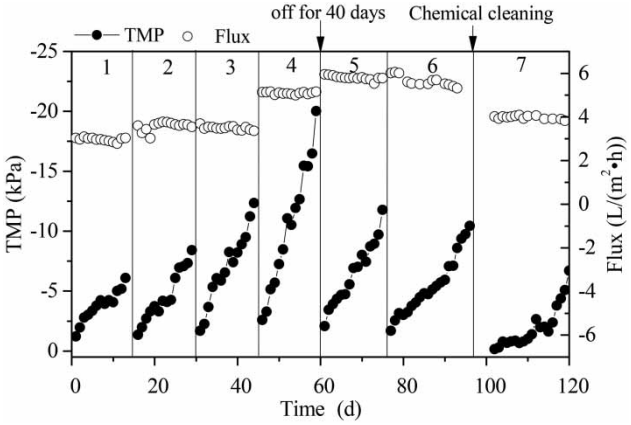

Figure 5 | TMP and membrane flux variation under different operation conditions.

rate increased rapidly during stages 1–3 with similar membrane flux. Thus, membrane fouling could be alleviated by regular physical cleaning in a short time, but other control measures were still needed for long term operation.

When the permeation/relaxation rate was decreased from 10/1 to 5/1 (stage 5 to stage 6), the steady operation time of the membrane module improved from 15 days to 20 days and the fouling rate was reduced by about 10%. Besides, the TMP increase rate in stage 6 was slower than stage 5 (Figure 5), which indicated the decreasing permeation/relaxation rate had a significant effect on slowing down membrane fouling. However, in terms of handling capacity, a decrease in the permeation/relaxation rate reduced the filtration efficiency by 8.3%. Thus, practical applications should consider the influent volume if the membrane fouling rate is controlled by adjusting the permeation/relaxation rate.

After 100 days of reactor operation, the filtration efficiency of the membrane module was recovered by chemical cleaning as follows: the membrane surface was washed with water to remove the adherent sludge, after which it was immersed first in NaClO (200 mg/L) and then in citric acid (125 mg/L) for 48 h, respectively. After a second wash with water, the membrane was immersed in water until the alkalinity of the water was >70 mg/L. After chemical cleaning, the membrane was operated steadily for 20 days and exhibited both a higher flux and a 60% decrease in the fouling rate compared to the first stage under the same operation conditions. This result indicated that the filtration capacity could be fully recovered by chemical cleaning in the early phase of membrane fouling, which was a very important reference for long term operation of the membrane module. A certain frequency of on-line chemical cleaning is very essential for long period operation, and the exact frequency and methods should be determined by the cleaning effect, cost, the influence on anaerobic degradation and on-site situations etc.

To further understand the membrane fouling mechanism, the membrane fouling rate was calculated at each stage and the corresponding changes in MLSS, EPS and SMP were analyzed. The linear correlation analysis identified MLSS and the polysaccharide contents of EPS as the direct cause of membrane fouling (Figure 6). Wu and Huang pointed out that an MLSS concentration higher than 10 g/L was considered to increase sludge viscosity, which may aggravate membrane fouling (Wu & Huang 2009). In this study, a high MLSS concentration of 32.3 ± 6.2 g/L can lead to formation of a sludge cake layer on the surface of the ultrafiltration membrane and cause resultant physical blocking. The effect of EPS/SMP on membrane fouling in AnMBRs is complex, and there were conflicting conclusions about the effect of protein and polysaccharide on membrane fouling (Meng *et al.* 2009). In this study, pore blocking by soluble macromolecules was probably not the main cause of fouling, since neither the SMP nor the protein concentration of the EPS showed an obvious correlation with the membrane fouling rate. And the reasonable explanation for this result is that the ultrafiltration hollow-fibre membrane used in this study has a pore size of 0.04 μm, which is too small for soluble macromolecules to enter and create pore blocking. Former studies also found that internal fouling caused by pore blocking could be the dominant mechanism in micro-filtration hollow-fiber membranes instead of ultra-filtration ones (Drews 2010; Lin *et al.* 2014).

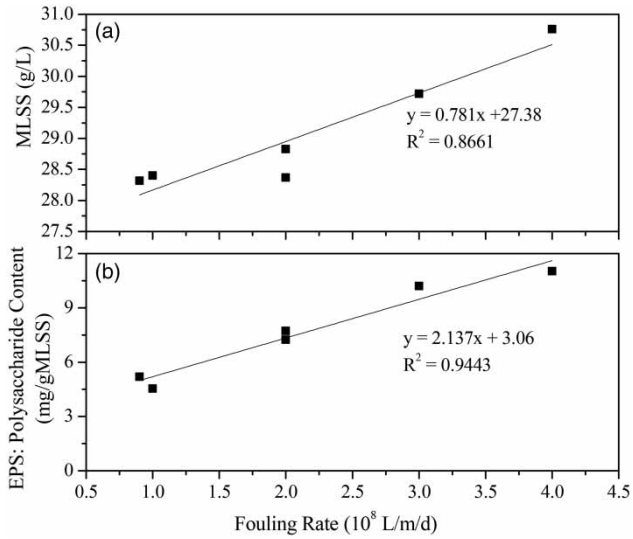

Figure 6 | Relationship between the fouling rate and both mixed liquor suspended solids (MLSS) and the polysaccharide content of the EPS.

Ammonia and phosphorus recovery

In this study, certain amounts of precipitates were observed in the bottom of the permeate collecting tank. And the average concentrations of NH_4^+-N and PO_4^{3+}-P of the collected permeate were 11 mg/L and 13.8 mg/L lower than those of the fermentation liquor, respectively. Considering the pH of the permeate was 7.9 ± 0.1, and contained magnesium (61.6 ± 7.8 mg/L) and calcium (47.7 ± 3.3 mg/L), ammonia and phosphorus precipitation might occur in the permeate. Therefore, recovery of ammonia and phosphorus from the permeate under different pH (8, 9, 10) were examined in this study.

Experimental results showed that the removal efficiency of phosphorus (24.7%, 70.5%, 86.5%) increased along with

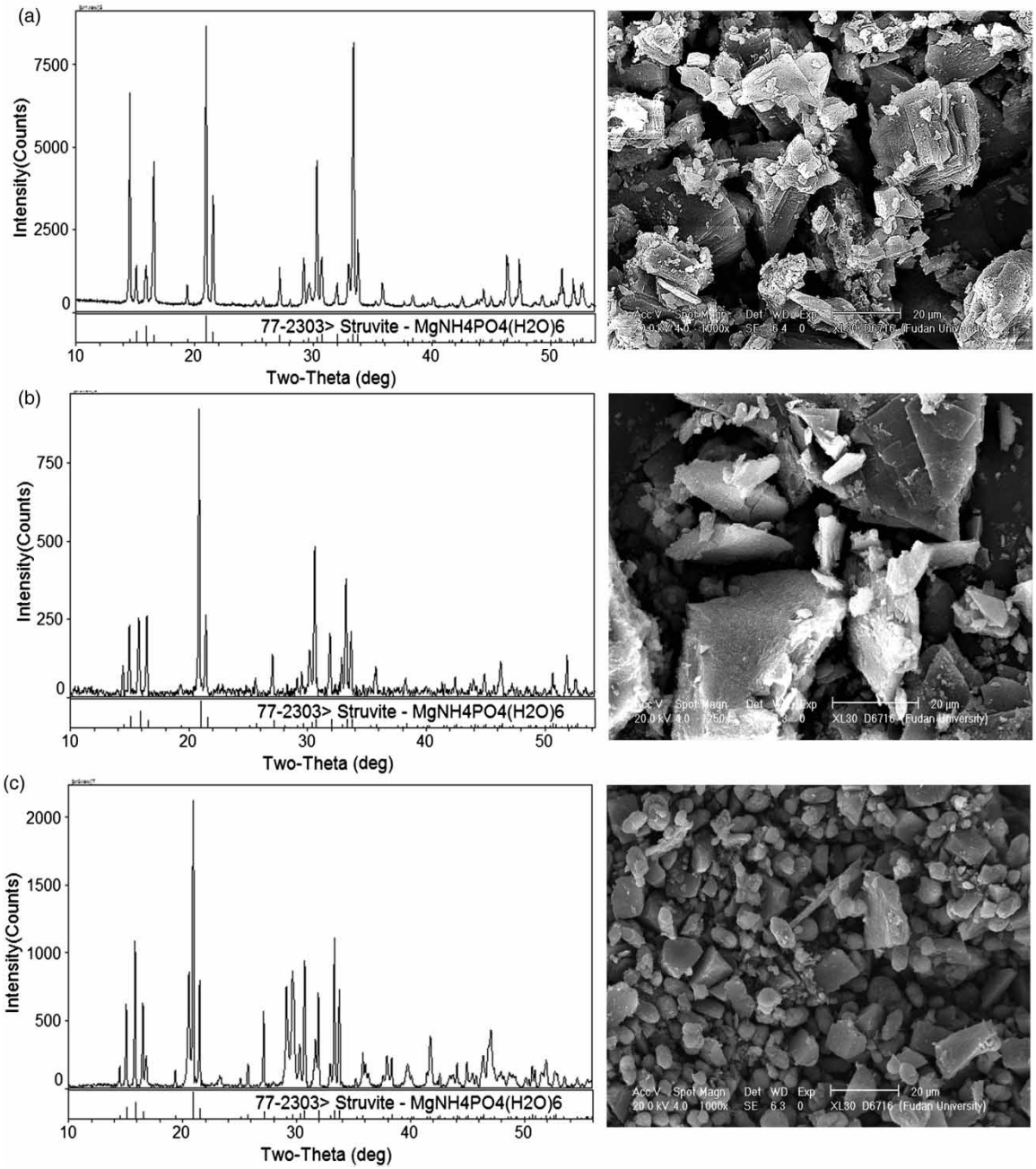

Figure 7 | XRD spectrograms and SEM photographs under different pH: (a) pH 8; (b) pH 9; (c) pH 10.

pH, while the highest removal efficiency of Mg^{2+} (21.8%) and Ca^{2+} (73.6%) was observed at pH 9 and 10 respectively. The results inferred that more calcic precipitates were formed under pH 10, and the struvite under pH 10 might have lower purity. The above speculation was confirmed by the XRD scanning and crystalline form analysis of the precipitates under three pH conditions (Figure 7). Results showed that precipitates of pH 8 and 9 both had high similarities with standard struvite crystal, which were 97% and 98% respectively. However, the precipitate of pH 10 had a low similarity of 74% with standard struvite crystal and showed 40% similarity with standard $Ca_2P_2O_7$ crystal. In addition to purity, crystal size also affects the value of struvite. According to the SEM photographs, the precipitates of pH 8 and 9 both were regular orthorhombic crystal like struvite and that of pH 9 had larger size, while that of pH 10 had no regular shape and small size. Thus, pH 9 was the optimum pH for nitrogen and phosphorus recovery as struvite in this study.

CONCLUSIONS

In this work, the feasibility of treating swine manure wastewater in an AnMBR and the recovery of ammonia and phosphorus in the permeate were investigated. The AnMBR system achieved steady operation under a high concentration of MLSS for 120 days, with a total COD removal efficiency of 96% and methane yield of 280 mL/gVS_{added}. The methane yield of the AnMBR is 83% higher than that of the single CSTR, which indicates further degradation of organic matters in the AnMBR system. Moreover, the relationship between membrane fouling rate and MLSS, EPS and SMP, and the effects of permeation/relaxation rate and physical, chemical cleaning on membrane fouling were discussed in this study. MLSS and the polysaccharide contents of the EPS were linearly correlated with membrane fouling rate, and thus considered to be the direct causes of membrane fouling. And a decrease in the permeation/relaxation rate together with chemical cleaning effectively reduced membrane fouling. Ammonia and phosphorus was recovered as struvite by crystallization at pH 8, 9 and 10, of which pH 9 was found to be optimum for struvite formation. The study established a two-step treatment procedure that combined the AnMBR and crystallization process for nutrient recovery from swine manure wastewater, which has a profound significance for resource recovery and utilization of high strength wastewater.

ACKNOWLEDGEMENT

This research was supported by GE CTC, National Natural Science Foundation of China (51178326, 51378373), State Key Laboratory of Pollution Control and Resource Reuse Foundation (No. PCCRE16015), and Fundamental Research Funds for the Central Universities.

REFERENCES

APHA 1998 *Standard Methods for the Examination of Water and Wastewater*, 20th edn. The American Public Health Association, Washington, DC, USA.

Chen, Y., Sun, B. S., Huang, X. & Zhang, B. 2009 Study of microbial population succession in MBR at different stages. *Chinese Journal of Environmental Engineering* **3** (6), 1023–1028.

Dagnew, M., Pickel, J., Paker, W. & Seto, P. 2013 Anaerobic membrane bio-reactors for waste activated sludge digestion: tubular versus hollow fiber membrane configurations. *Environmental Progress & Sustainable Energy* **32** (3), 598–604.

Drews, A. 2010 Membrane fouling in membrane bioreactors – characterisation, contradictions, cause and cures. *Journal of Membrane Science* **363** (1–2), 1–28.

Kim, J., Kim, K., Ye, H., Lee, E., Shin, C., McCarty, P. L. & Bae, J. 2011 Anaerobic fluidized bed membrane bioreactor for wastewater treatment. *Environmental Science & Technology* **45** (2), 576–581.

Lee, S. M., Jung, J. Y. & Chung, Y. C. 2001 Novel method for enhancing permeate flux of submerged membrane system in two-phase anaerobic reactor. *Water Research* **35** (2), 471–477.

Lin, H. J., Zhang, M. J., Wang, F. Y., Meng, F. G., Liao, B. Q., Hong, H. C., Chen, J. R. & Gao, W. J. 2014 A critical review of extracellular polymeric substances (EPSs) in membrane bioreactors: characteristics, roles in membrane fouling and control strategies. *Journal of Membrane Science* **460**, 110–125.

Lopez-Fernandez, R., Aristizabal, C. & Irusta, R. 2011 Ultrafiltration as an advanced tertiary treatment of anaerobically digested swine manure liquid fraction: a practical and theoretical study. *Journal of Membrane Science* **375** (1–2), 268–275.

Lyko, S., Wintgens, T., Al-Halbouni, D., Baumgarten, S., Tacke, D., Drensla, K., Janot, A., Dott, W., Pinnekamp, J. & Melin, T. 2008 Long-term monitoring of a full-scale municipal membrane bioreactor – characterisation of foulants and operational performance. *Journal of Membrane Science* **317** (1–2), 78–87.

Meng, F., Chae, S. R., Drews, A., Kraume, M., Shin, H. S. & Yang, F. L. 2009 Recent advances in membrane bioreactors (MBRs): membrane fouling and membrane material. *Water Research* **43** (6), 1489–1512.

Nasir, I. M., Ghazi, T. I. Mohd. & Omar, R. 2012 Bioreactor performance in the anaerobic digestion of cattle manure: a

review. *Energy Sources, Part A: Recovery, Utilization, and Environmental Effects* **36** (13), 1476–1483.

Nishiyama, T., Ueki, A., Kaku, N., Watanabe, K. & Ueki, K. 2009 Bacteroides graminisolvens sp nov., a xylanolytic anaerobe isolated from a methanogenic reactor treating cattle waste. *International Journal of Systematic and Evolutionary Microbiology* **59**, 1901–1907.

Niu, Q. H., Kobayashi, T., Takemura, Y., Kubota, K. & Li, Y. Y. 2015 Evaluation of functional microbial community's difference in full-scale and lab-scale anaerobic digesters feeding with different organic solid waste: effects of substrate and operation factors. *Bioresource Technology* **193**, 110–118.

Padmasiri, S. I., Zhang, J., Fitch, M., Norddahl, B., Morgenroth, E. & Raskin, L. 2007 Methanogenic population dynamics and performance of an anaerobic membrane bioreactor (AnMBR) treating swine manure under high shear conditions. *Water Research* **41** (1), 134–144.

Rajagopal, R., Massé, D. I. & Singh, G. 2013 A critical review on inhibition of anaerobic digestion process by excess ammonia. *Bioresource Technology* **143**, 632–641.

Rosenberger, S., Laabs, C., Lesjean, B., Gnirss, R., Amy, G., Jekel, M. & Schrotter, J. C. 2006 Impact of colloidal and soluble organic material on membrane performance in membrane bioreactors for municipal wastewater treatment. *Water Research* **40** (4), 710–720.

Shen, L., Zhou, Y., Mahendran, B., Bagley, D. M. & Liss, S. N. 2010 Membrane fouling in a fermentative hydrogen producing membrane bioreactor at different organic loading rates. *Journal of Membrane Science* **360** (1–2), 226–233.

Ueki, A., Abe, K., Kaku, N., Watanabe, K. & Ueki, K. 2008 Bacteroides propionicifaciens sp nov., isolated from rice-straw residue in a methanogenic reactor treating waste from cattle farms. *International Journal of Systematic and Evolutionary Microbiology* **58**, 346–352.

Wang, Z., Wu, Z., Yu, G., Liu, J. & Zhou, Z. 2006 Relationship between sludge characteristics and membrane flux determination in submerged membrane bioreactors. *Journal of Membrane Science* **284**, 87–94.

Wang, W., Xie, L., Chen, J., Luo, G. & Zhou, Q. 2011 Biohydrogen and methane production by co-digestion of cassava stillage and excess sludge under thermophilic condition. *Bioresource Technology* **102**, 3833–3839.

Weiland, P. 2006 Biomass digestion in agriculture: a successful pathway for the energy production and waste treatment in Germany. *Engineering in Life Sciences* **6** (3), 302–309.

Wu, J. L. & Huang, X. 2009 Effect of mixed liquor properties on fouling propensity in membrane bioreactors. *Journal of Membrane Science* **342** (1–2), 88–96.

Xie, L., Chen, J., Wang, R. & Zhou, Q. 2012 Effect of carbon source and COD/NO_3^- -N ratio on anaerobic simultaneous denitrification and methanogenesis for high-strength wastewater treatment. *Journal of Bioscience and Bioengineering* **113**, 759–764.

Xu, M., Wen, X., Yu, Z., Li, Y. & Huang, X. 2011 A hybrid anaerobic membrane bioreactor coupled with online ultrasonic equipment for digestion of waste activated sludge. *Bioresource Technology* **102** (10), 5617–5625.

First received 10 February 2017; accepted in revised form 25 April 2017. Available online 9 May 2017